Chinese Journal of Polymer Science Vol. 31, No. 5, (2013), 737–747

Chinese Journal of Polymer Science
© Chinese Chemical Society
Institute of Chemistry, CAS
Springer-Verlag Berlin Heidelberg 2013

PARTICLE-COLLISION AND POROGEN-LEACHING TECHNIQUE TO FABRICATE POLYMERIC POROUS SCAFFOLDS WITH MICROSCALE ROUGHNESS OF INTERIOR SURFACES*

Zhen Pan, Ze-hua Qu, Zheng Zhang, Rong Peng, Ce Yan and Jian-dong Ding**
State Key Laboratory of Molecular Engineering of Polymers, Department of Macromolecular Science, Laboratory of Advanced Materials, Fudan University, Shanghai 200433, China

Abstract A facile technique is herein reported to fabricate three-dimensional (3D) polymeric porous scaffolds with interior surfaces of a topographic microstructure favorable for cell adhesion. As demonstration, a well-known biodegradable polymer poly(lactide-*co*-glycolide) (PLGA) was employed as matrix. Under the porogen-leaching strategy, the large and soft porogens of paraffin were modified by colliding with small and hard salt particles, which generated micropits on the surfaces of paraffin spheres. The eventual PLGA scaffolds after leaching the modified porogens had thus interior surfaces of microscale roughness imprinted by those micropits. The microrough scaffolds were confirmed to benefit adhesion of bone marrow stromal cells (BMSCs) of rats and meanwhile not to hamper the proliferation and osteogenic differentiation of the cells. The insight and technique might be helpful for biomaterial designing in tissue engineering and regenerative medicine.

Keywords: Tissue engineering; Porous scaffolds; Surface topography; Cell adhesion; Poly(lactide-*co*-glycolide) (PLGA).

Electronic Supplementary Material Supplementary material is available in the online version of this article at http://dx.doi.org/10.1007/s10118-013-1264-1.

INTRODUCTION

Porous scaffolds play an important role in tissue engineering and regenerative medicine[1–4]. So far the importance of cell-material interactions for biomaterial studies has been well recognized, and a scaffold is for not only loading cells but also probably influencing cell behaviors. Several chemical and physical cues of material surfaces have been revealed to regulate cell responses[5–16]. A simple but practical physical cue is surface topography. Progress has been made in examinations of topographical effects on cell responses[17–37]. To control topography is thus very meaningful for biomaterial design.

While most of pertinent researches have been made on two dimensional substrates, techniques to generate microscale roughness in the interior surfaces of three-dimensional (3D) porous scaffolds are strongly called for. Herein the authors report a technique to fabricate 3D scaffolds with interior surfaces of pre-designed microscale topography favorable for cell adhesion. Poly(lactide-*co*-glycolide) (PLGA) was employed as the model matrix. This is a very popular biodegradable polymer[38–44], and porous scaffolds composed of PLGA are frequently used in tissue engineering. The pores in 3D scaffolds can be generated by several ways and most commonly by the strategy of porogen leaching[38, 45–48].

* This work was financially supported by Chinese Ministry of Science and Technology (973 programs Nos. 2009CB930000 and 2011CB606203), and NSF of China (Nos. 21034002, 91127028 and 51273046).
** Corresponding author: Jian-dong Ding (丁建东), Email: jdding1@fudan.edu.cn
Invited paper dedicated to Professor Fosong Wang on the occasion of his 80th birthday
Received November 26, 2012; Revised December 20, 2012; Accepted December 24, 2012
doi: 10.1007/s10118-013-1264-1

Under this strategy, a technique to prepare porogens of a microtextured surface was developed and then the desired porous scaffold was fabricated in this study with the procedure schematically presented in Fig. 1. The original approach to use paraffin spheres as porogens to fabricate tissue engineering scaffolds was suggested by the group of Ma[39], and confirmed by other groups[49, 50]. The innovation in the present study comes from preparation of paraffin spheres of micropits on their surfaces, assisted by salt particulates. It should be indicated that although salt particulates of 100–400 μm have been widely used to fabricate tissue engineering scaffolds[38, 51], the particles have herein a different size and function. Those salt particulates were employed by the authors just for colliding with the soft paraffin spheres of diameter about 300–450 μm in order to generate micropits on the surface of paraffin porogens, and the salt particulates as the surface modifier were quite small, just about 1–15 μm.

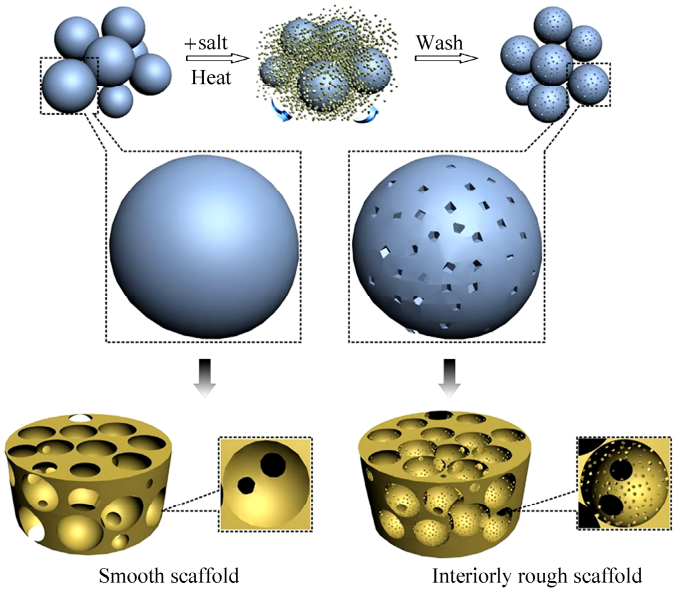


Fig. 1 Schematic presentation of fabrication of 3D PLGA porous scaffolds with interior surfaces of microroughness (interiorly rough scaffold) as well as PLGA scaffolds with a relatively smooth interior surfaces (smooth scaffold)
The strategy of porogen leaching was used to fabricate scaffolds, and paraffin spheres of diameter about 300–450 μm served as porogens. In preparation of porogens with micropits, paraffin spheres were mixed with small salt particulates, and the mixture was heated and stirred as indicated in the first row; the soft paraffin spheres were imprinted by hard and small salt particulates, as indicated in the second row. The micropits on the surfaces of porogens led to microroughness on the interior surfaces of the resulting "interiorly rough scaffold", while using the virgin paraffin spheres as porogens led to the "smooth scaffold".

Besides observation of the surface morphology of the PLGA scaffolds, the authors also examined adhesion, proliferation and osteogenic differentiation of bone marrow stromal cells (BMSC) of rats on the pore surfaces. The present work thus distinguishes itself from the previous publications *via* the following issues: (1) a facile approach to fabricate a porous PLGA scaffold with pre-designed micro-topography of the interior surface based upon the novel particle-collision and porogen-leaching technique, (2) *in vitro* study of cell responses on microscale topography in the interior of the 3D scaffolds.

EXPERIMENTAL

Materials

Poly(lactide-*co*-glycolide) with 85:15 molar ratio of L-lactide and glycolide (PLGA85/15) from Purac Inc. (Netherlands) was used as the scaffold matrix material. The copolymer had the number average molecular

weight 3.59×10^5 and the polydispersity index 1.72. The porogens were composed of paraffin. The paraffin had a melting range of 58–60 °C. The porogen modifiers were composed of sodium chloride. The salt was of the analytical grade.

Preparation of Paraffin Porogens of Surface Roughness

Paraffin microspheres of diameter 300–450 μm were prepared by quenching the associated emulsion in ice water[50]. In order to obtain the modified porogens in the present work, the authors also prepared sodium chloride particles of 1–15 μm by smashing salt granules in a high-speed disintegrator. Then, 10 g paraffin sphere was mixed with 100 g salt particles in a flask. The mixture was heated to 40–60 °C and was mechanically stirred at 200 r/min for half an hour. The resulting mixture was immediately poured into 500 mL solvent of deionized water and ethanol (deionized water:ethanol = 1:1) for 5 min, and subsequently rinsed with the mixture solvent for several times. Novel paraffin spheres of rough surfaces *via* the particle-collision technique were collected after dried.

Fabrication of Porous PLGA Scaffolds

The room-temperature compression molding/porogen leaching approach was employed to fabricate porous scaffolds. First, 2 g granular PLGA85/15 was dissolved in 11 mL dichloromethane to form a polymer solution. Then, a composite of the porogens and the polymer solution was prepared, and pressed into a mould of an inner diameter 10 mm and a height 10 mm. The compressive pressure was exerted by screws in hand to keep the mold. After 24 h, we released the sample from the mould. The residual organic solvent was distilled in the air. Then, Soxhlet extractor with *n*-pentane was used as the refluxing solvent to leach paraffin microspheres. The porous scaffolds were air-dried for 24 h and then freeze-dried for another 48 h. The resulting scaffolds were stored in a desiccator under vacuum.

The porosity (φ_v) of the scaffolds was determined by a modified liquid replacement method[52]. Ethanol was used as a replacement liquid to determine the volume of pores. The porosities of all scaffolds in the experiments were about 90%.

Characterization of Porogens and 3D Scaffolds

Scanning electronic microscopy (SEM) was used to observe paraffin spheres, and slices of 3D scaffolds. The samples were coated with gold prior to observations. The electric voltage was set as 20 kV in the electronic microscope.

Cell isolation and Culture

Neonatal Sprague Dawley (SD) rats were used to isolate BMSCs. After sacrificing the rats by cervical dislocation, femurs and tibias were removed, and the marrow was flushed out, centrifuged, and resuspended in low-glucose Dulbecco's modified Eagle medium (DMEM, Gibco) supplemented with 10% fetal bovine serum (FBS, Gibco). Then cells were cultured in humidified incubator at 37 °C with a 5% CO_2 atmosphere. Non-adherent cells were removed after 2 days. BMSCs of the early passage were used for later experimental studies.

The PLGA scaffolds were prewetted in 70% ethanol for 2 h to sterilize and enhance the water uptake. The scaffolds were immersed into phosphate buffer saline (PBS) for 30 min to remove ethanol. After repeating such a replacement 6 times, the authors immersed the scaffolds into culture medium twice, each time for 2 h. Scaffold slices were placed into 12-well tissue culture plates (TCP) prior to cell seeding.

BMSCs in the growth medium were seeded to the PLGA scaffolds with 20×10^4 cells into one scaffold. It has been revealed from cell culture on 2D surfaces that the initial cell density influences cell differentiation[53, 54]. The seeding density in the experiment was equivalent to about 1.2×10^4 cells per cm^2, which is moderate and appropriate for the present studies. The cell-loaded scaffold slices of 10 mm diameter and 2 mm thickness in 12-well plates with their bottoms covered by agar were put into the incubator for 4 h to allow the cells to attach on the pore surfaces of the scaffolds. Then, an additional 1.5 mL of the primary culture medium was added to each well.

A scanning electronic microscope (TS 5136MM) was used to observe the morphology of cells after being cultured in the scaffolds for 6 h. The cells were fixed in 4% paraformaldehyde for 1 h, dehydrated in a graded series of ethanol solution (30%, 50%, 70%, 90%, 100%, *V*/*V*) for 30 min each time. The scaffolds were dried and then sputtered with gold. Sample imaging was operated at 20 kV.

MTT Assay

Cell viability was estimated by a 3-(4,5-dimethylthiazol-2-yl)-2,5-diphenyltetrazolium bromide (MTT) assay. After cell culture for 24 or 72 h, the growth medium containing 0.5 mg/mL MTT solution was added. 4 h later, the upper medium was removed, and dimethyl sulfoxide (DMSO) was added to dissolve the intracellular formazan. For the control group in TCP, the same amount of DMSO was added as well. The absorbance of the samples was detected in a microplate spectrophotometer (Thermo Multiscan MK3) at 492 nm.

Osteogenic Differentiation of BMSCs in Scaffolds

An osteogenic medium was used to replace the culture medium to induce the differentiation of BMSCs towards the osteogenic phenotype. The osteogenic medium contained 50 mmol/L ascorbic acid-2-phosphate, 10 mmol/L β-glycerophosphate and 100 nmol/L dexamethasone as well as the high-glucose DMEM (Sigma). PLGA scaffold slices were of 10 mm diameter and 2 mm height. During the 6 days of induction, the medium was replaced every 2 days.

Measurements of the Cell Number of BMSCs

The fluorometric analysis of DNA content using Hoechst 33258 (Sigma) was used to measure the cell number in the scaffolds[55]. A solution of highly polymerized calf thymus DNA of 50 μg/mL and solutions of DNA stock of 0, 20, 40, 60, 80, 100, 120, 140 and 160 μL were prepared to calibrate the DNA standard curve. The scaffolds and DNA standards were immersed into 1.4 mL of 10 mmol/L ethylenediaminetetraacetic acid (pH 12.3) and then put in a 37 °C bath for 20 min. After cooling on ice for 5 min, 0.2 mL of 1 mol/L KH_2PO4 was added to neutralize each solution. Scaffolds or DNA standards were mixed with 1.5 mL of a 100 ng/mL solution of the Hoechst 33258 dye in 100 mmol/L NaCl and 10 mmol/L Tris buffer (pH 7.0) overnight. The fluorescence of 2.5 mL solution was detected in a fluorescence spectrophotometer (Cary Eclipse, VARIAN), upon excitation at 350 nm and emission at 455 nm. The fluorescence intensity was used to calculate, based on the DNA standard curve, the total mass of DNA, which was further converted to the cell number following the conversion factor reported in the literature[56].

Activity of Alkaline Phosphatase

After the osteogenic induction, the alkaline phosphatases (ALP) in the cells were stained using Sigma kit 85L1 following the manufacturer's instruction. Cells were fixed in acetone/citrate, rinsed in PBS, and stained with Fast Blue RR/naphthol. The pigment formed at the sites of ALP activity was dissolved in tetrahydrofuran, and the final detection was performed in a microplate spectrophotometer (Thermo Multiscan MK3) at 570 nm after dilution to keep the values of optical density (OD) in a range linearly related to the formazan concentration. Independent parallel samples were joined in statistics ($n = 4$).

Statistical Analysis

Data sets were compared using Student *t*-test, with $p < 0.05$ as the criterion of a significant difference. If the total ALP activity in each slice of scaffold and the associated cell number per slice were x_1 and x_2, the mean value of ALP activity per cell was obtained by $\overline{x}_1 / \overline{x}_2$, and $s_{(x_1/x_2)} = \sqrt{s_{x_1}^2 \overline{x}_2^2 + s_{x_2}^2 \overline{x}_1^2} / \overline{x}_2^2$ gave the associated standard deviation.

RESULTS

Preparation of Spherical Porogens of Micro-concave Surfaces

In order to fabricate 3D PLGA scaffolds, the authors suggested an approach to prepare paraffin spheres of micropitted surfaces with the principle presented in Fig. 1. Virgin paraffin spheres of diameters of 300–450 μm were first prepared. Granular sodium chloride was also smashed with a high-speed disintegrator to obtain the salt

particles of size 1–15 μm, and then mixed with paraffin. The mixtures of two kinds of particles were then heated under stirring, and the surfaces of paraffin spheres were imprinted by the small salt particles to generate micropits. Typical results of paraffin spheres are shown in Fig. 2. While the paraffin surface without the salt collision was relatively smooth (Figs. 2a and 2c), a concave surface was observed if the paraffin spheres were treated by the small salt particles *via* the particle-collision technique at 50 °C (Figs. 2b and 2d).

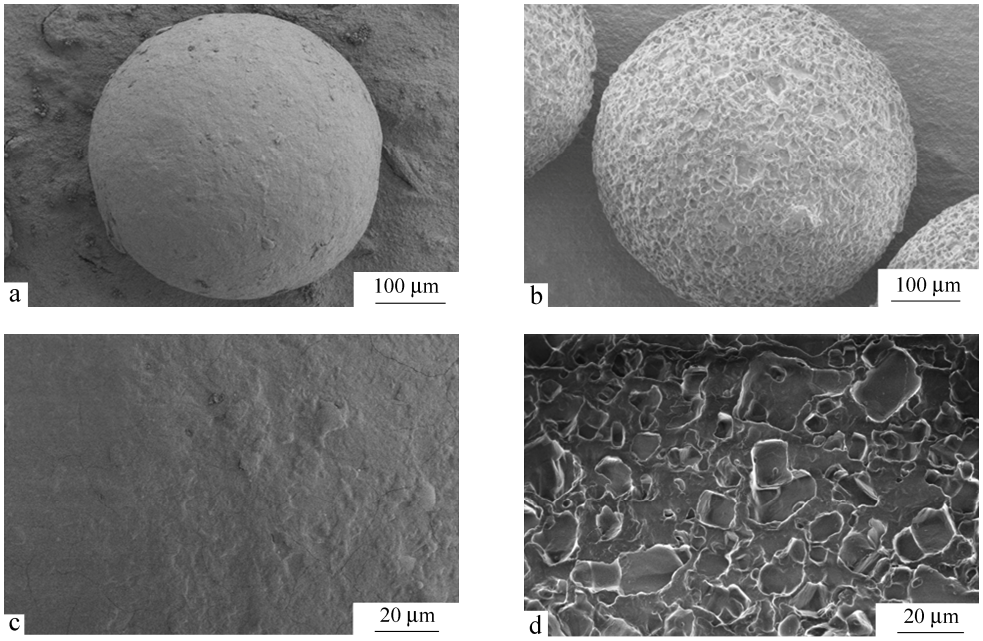


Fig. 2 SEM micrographs of paraffin spheres of a smooth surface (a) and rough surface (b) and their magnified images (c and d)
The concave paraffin spheres were modified at 50 °C.

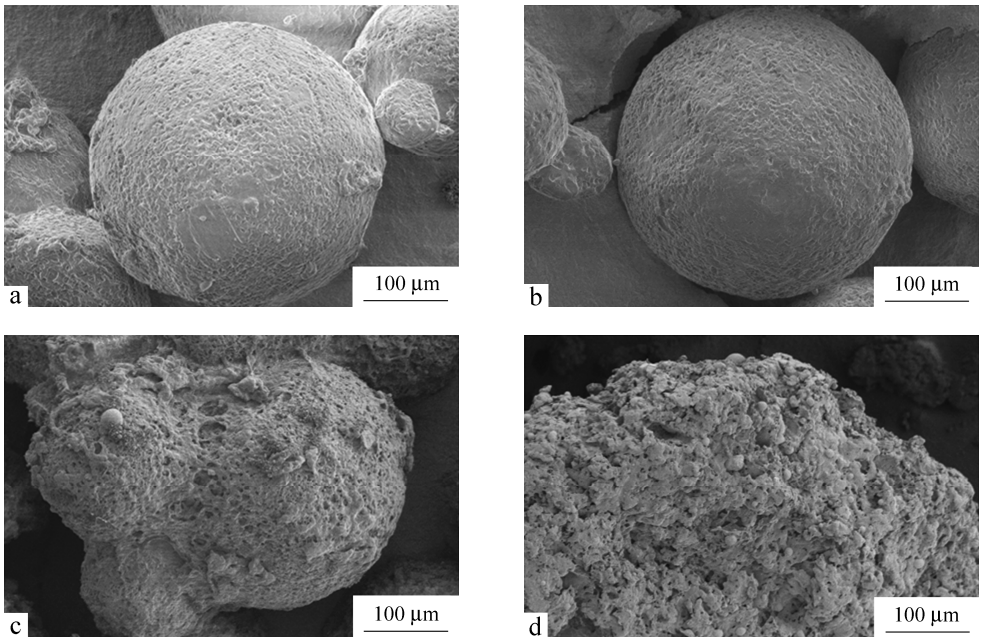


Fig. 3 SEM micrographs of paraffin spheres modified at different temperatures: (a) 40, (b) 45, (c) 55 and (d) 60 °C

The imprinting happened during collision of the hard salt particles and the soft paraffin spheres. The particle mixture was heated to soften the paraffin. It is noteworthy that a successful preparation using such a particle-collision technique is dependent upon an appropriate softening temperature. Some unsuccessful cases are shown in Fig. 3. At 40 °C (Fig. 3a) and 45 °C (Fig. 3b), only a few micropits were produced on the paraffin surfaces. Significant micropits were achieved when the preparation temperature was set at 50 °C (Figs. 2b and 2d). The paraffin spheres got to stick to each others at higher temperatures, and even melted at 60 °C (Fig. 3d).

Fabrication of 3D Porous Scaffolds with Interior Surfaces of Microroughness

After compression molding and particulate leaching, the micropits on the porogen surfaces were transferred into the pore walls of scaffolds, and turned into microroughness, as shown in Fig. 4. The novel concave spheres in the present experiment play roles of not only a porogen but also a modification agent of surface topography.

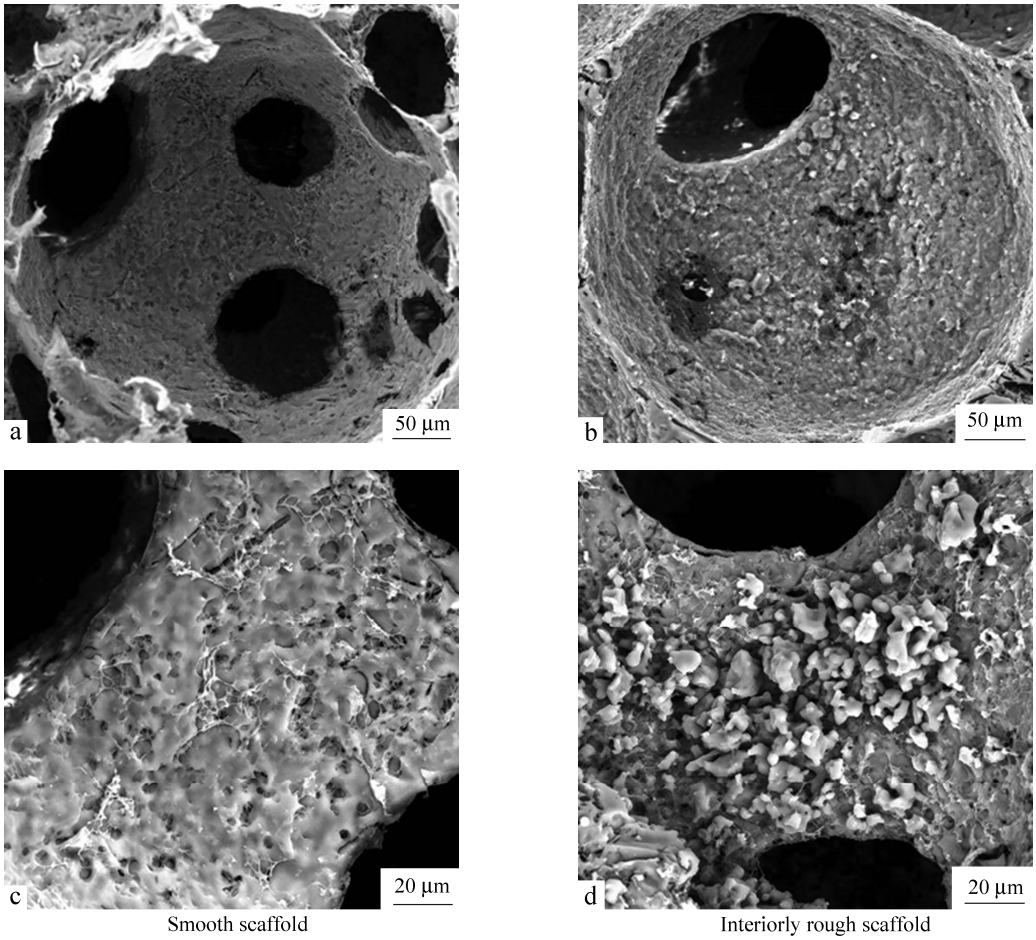


Fig. 4 SEM micrographs of PLGA scaffolds fabricated using virgin paraffin spheres as porogens (a, c) and modified spheres of a micro-concave surface as porogens (b, d)
The micro-concave surfaces of the paraffin spheres led to micro-convex rough interior surfaces of the porous scaffolds.

SEM micrographs of cross-sections of PLGA porous scaffolds fabricated using 90 vol% concave paraffin spheres as porogens of 300–450 μm are shown in Fig. 4, together with the micrographs of "smooth scaffold" using traditional paraffin spheres as porogens. It should be indicated that even the so-called smooth scaffold cannot have a perfect smooth interior surface, due to the inherent roughness of the virgin paraffin porogens and

also due to minor pores generated during solvent evaporation in scaffold fabrication[39, 50]. Nevertheless, a relative rougher surface with some micro-convexity is seen in Figs. 4(b) and 4(d) for the "rough scaffold", which is reminiscent of the concave paraffin spheres imprinted by the small salt particles.

Cell Adhesion and Proliferation in 3D Porous Scaffolds of Relatively Smooth or Rough Interior Surfaces

BMSC cells adhered and spread in the PLGA scaffolds as shown in Fig. 5. Pseudopodials of the cells preferred anchoring those micro-convexities. Comparison between the two kinds of scaffolds was also made from quantitative measurements. The seeding efficiencies were very similar between the two scaffolds, as illustrated in Fig. S1 in Supporting Information. Yet, better adhesion of BMSCs on microrough surfaces of the PLGA porous scaffolds was revealed by the MTT assay, as shown in Fig. 6.

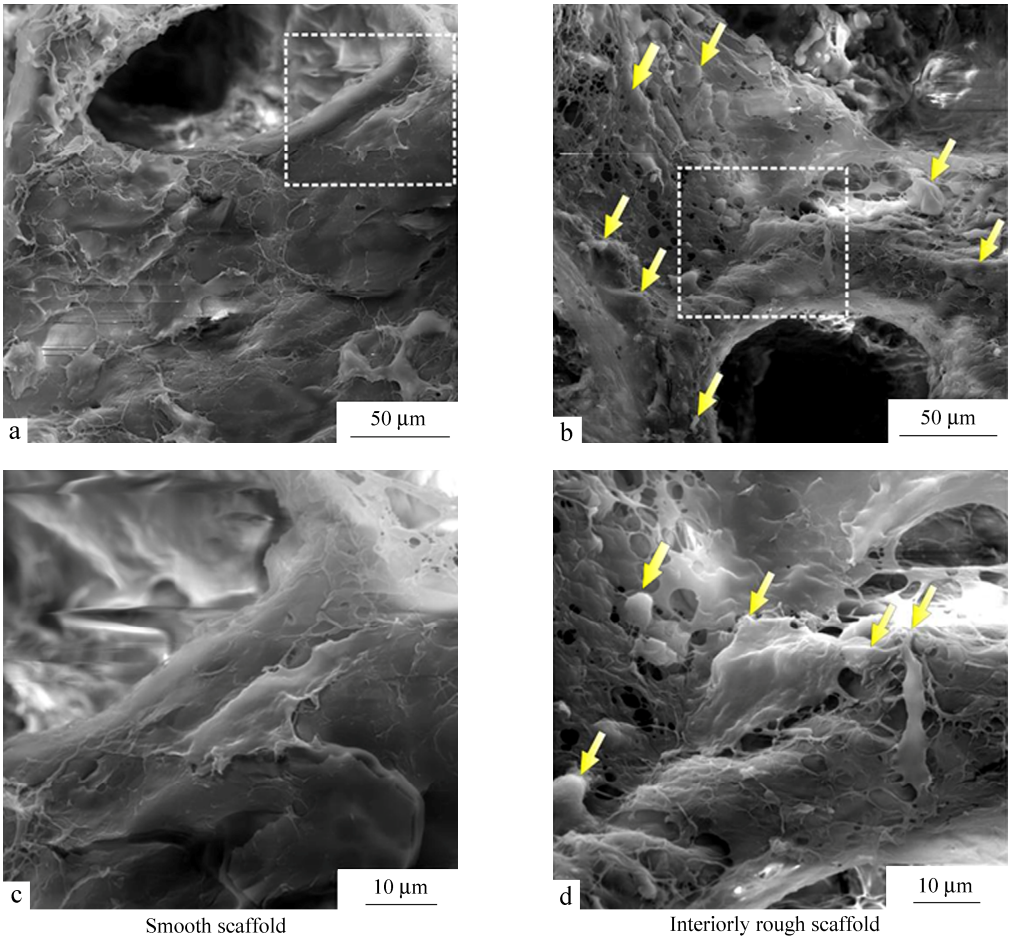


Fig. 5 SEM micrographs of BMSCs on the interior surfaces of PLGA scaffolds fabricated by virgin paraffin spheres (a, c) and salt-imprinted paraffin spheres (b, d)
The arrows in (b) and (d) indicate some micro-convexities on interior surfaces of the scaffold.

Proliferation rates were calculated, with the results shown in Fig. S2. The surface microroughness did not obstruct the proliferation of the adherent cells. So, after combining both cell adhesion and proliferation, it could be stated that our 3D scaffolds provided the interior surfaces relatively beneficial for cell responses.

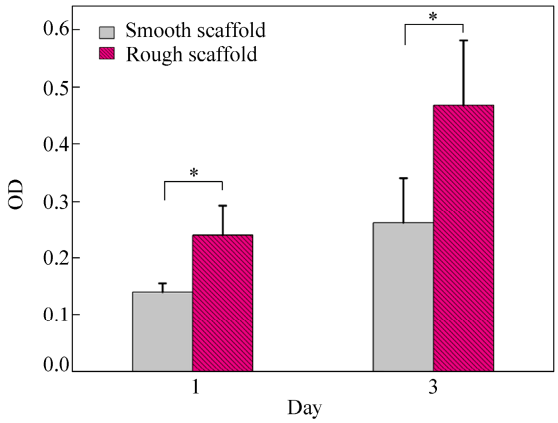


Fig. 6 MTT measurements of viability of BMSC cells on the scaffolds using the novel concave paraffin spheres compared with using the common smooth paraffin spheres as porogens ($n = 4$)
The p values from t-tests are listed in Table S1. The "*" indicates a significant difference with $p < 0.05$.

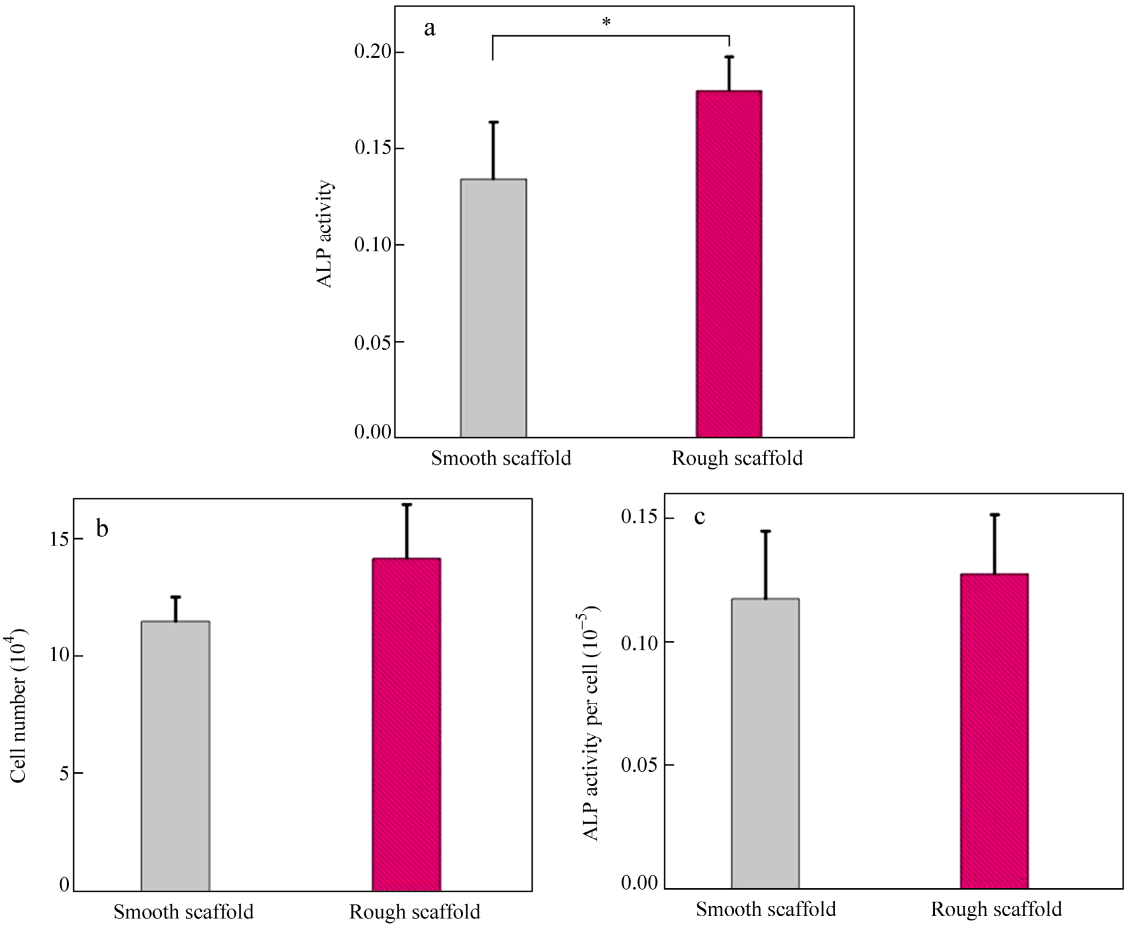


Fig. 7 Capability of osteogenic differentiation in the 3D PLGA scaffolds after 6 days in the osteogenic induction medium: (a) ALP activity per scaffold, (b) cell number of BMSCs per scaffold and (c) ALP activity per cell ($n = 4$)
The p values for Figs. 7(a)–7(c) are, respectively, listed in Tables S2–S4 in Supplementary information. A significant difference was found for ALP activity between the two groups in (a); the difference in (b) for cell number is relatively larger than in (c) for reduced ALP activity.

Osteogenic Differentiation of BMSCs in Porous Scaffolds of Smooth or Rough Surfaces

Cell differentiation in 3D porous scaffolds was further examined. After seeding BMSCs to scaffolds, an osteogenic differentiation was induced by immersing the scaffolds into the induction medium. After 6 days, the authors quantified ALP activity, with results shown in Fig. 7. Significant higher ALP levels were seen in the group of rough scaffolds (Fig. 7a). The normalized ALP activity (Fig. 7c) illustrated that the microroughness of the scaffolds neither suppressed nor enhanced osteogenic differentiation per cell. So, the increase of ALP levels per scaffold in Fig. 7(a) might mainly be contributed by the increase of cell number (Fig. 7b) due to better cell adhesion.

DISCUSSION

The last decade has witnessed much progress in revealing effects of microstructured topography on cell responses[18–20, 32, 57]. Most of previous studies are about cell responses on 2D or quasi-3D substrates. Since 3D scaffolds with microstructured surfaces play important roles in development of tissue engineering[26], interior surface topography in large 3D scaffolds should be adjusted and investigated. Our present report is focused upon the interior surfaces of microscale roughness. However, it is hard to develop large 3D scaffolds with well-defined interior surface microstructures. Attempts have been made to incorporate surface topographies onto the pore wall *via* stacking multiple layers[26] and 3D printing[58]. The stacking technique is very elegant, but time consuming for thick scaffolds; 3D printing relies on expensive equipments. On the other hand, most of the present surface modification techniques are difficult to be applied to control the topography of the interior surfaces in large 3D scaffolds. So, a simple and efficient technique to fabricate a 3D porous material with pre-defined microroughness on the interior surfaces *via* the approach of particle collision and porogen leaching has its own right, although one fabrication approach cannot replace another one.

The present work put forward a facile technique to fabricate porogen-induced polymeric porous scaffolds of interior microroughness, as schematically presented in Fig. 1. The authors prepared spheres with micropits on the surfaces. The resultant spheres played roles of both porogens and surface-modification agents. Using those paraffin spheres of micropits on the surfaces (Figs. 2b and 2d), we fabricated porous scaffolds with microroughness on the interior surfaces (Figs. 4b and 4d). The traditional paraffin spheres are of relatively smooth surfaces, as seen in Figs. 2(a) and 2(c). To obtain micropits on the surfaces of the porogens, the virgin porogens should be treated by a creative but practical approach. The authors eventually invented a collision way. First, cubic granular sodium chloride was smashed into salt particles of diameter 1–15 μm. Then the large paraffin spheres and small salt particles were mixed and stirred. The salt particles collided with the paraffin spheres, generating micropits on the paraffin surfaces *via* the particle-collision technique (Figs. 2b and 2d). In the process of scaffold fabrication, those micropits were incorporated onto the pore walls during mixing the porogen and PLGA solution, especially under pressing in the molding process. After the porogen leaching, the surfaces of the interior pores obtained pre-designed microroughness (Figs. 4b and 4d).

MTT arrays at 1 and 3 days (Fig. 6) and the proliferation rate (Fig. S2) illustrated that the rough scaffolds provided superior adhesion compared with the smooth scaffolds while not influencing the proliferation. The increase of the total ALP activity in the rough scaffolds was also found (Fig. 7a). Since ALP activities per cell were similar between the two scaffolds (Fig. 7c), the change of the total ALP activity per scaffold (Fig. 7a) and of the cell number (Fig. 7b) might mainly be contributed by the initial cell adhesion. The mechanism of the enhanced cell adhesion on surfaces of microroughness on the molecular level is still open.

CONCLUSIONS

In the present studies, the authors performed parallel fabrications of 3D porous PLGA scaffolds of the surfaces with the pre-designed microscale topography and the relatively smooth surfaces. Microroughness was, under the strategy of porogen leaching, introduced into the 3D scaffolds by successfully preparing rough paraffin porogens. The surface modification of the porogens were achieved *via* the novel particle-collision technique,

namely, colliding softened paraffin spheres by small and hard salt crystals under appropriate temperatures. The microroughness was found to enhance adhesion of BMSCs in the scaffolds while neither cell proliferation nor the osteogenic differentiation per cell was negatively influenced. The present research highlights the importance of surface topography in 3D scaffolds on cell behaviors and put forward a facile technique to modify the topography of the interior surfaces of 3D scaffolds, which is stimulating for the scaffold design in tissue engineering and tissue induction.

REFERENCES

1 Langer, R. and Vacanti, J.P., Science, 1993, 260: 920
2 Karageorgiou, V. and Kaplan, D., Biomaterials, 2005, 26(27): 5474
3 Wang, W., Li, D., Wang, M.C., Li, Y.L. and Gao, C.Y., Chinese. J. Polym. Sci., 2011, 29(2): 233
4 Ke, J.H., Wang, Z.K., Li, Y.Z., Hu, Q.L. and Feng, J., Chinese. J. Polym. Sci., 2012, 30(3): 436
5 Jiao, Y.P. and Cui, F.Z., Biomed. Mater., 2007, 2(4): R24
6 Zhang, C., Hu, Y.Y., Cui, F.Z., Zhang, S.M. and Ruan, D.K., Biomed. Mater., 2006, 1(2): 56
7 Curran, J.M., Chen, R. and Hunt, J.A., Biomaterials, 2005, 26(34): 7057
8 Benoit, D.S.W., Schwartz, M.P., Durney, A.R. and Anseth, K.S., Nature Mater., 2008, 7(10): 816
9 Huang, J.H., Grater, S.V., Corbellinl, F., Rinck, S., Bock, E., Kemkemer, R., Kessler, H., Ding, J.D. and Spatz, J.P., Nano Lett., 2009, 9(3): 1111
10 Zhang, Z., Lai, Y.X., Yu, L. and Ding, J.D., Biomaterials, 2010, 31(31): 7873
11 Tang, J., Peng, R. and Ding, J.D., Biomaterials, 2010, 31(9): 2470
12 Haque, A., Hexig, B., Meng, Q., Hossain, S., Nagaoka, M. and Akaike, T., Biomaterials, 2011, 32(8): 2032
13 Yan, C., Sun, J. and Ding, J., Biomaterials, 2011, 32(16): 3931
14 Peng, R., Yao, X. and Ding, J., Biomaterials, 2011, 32(32): 8045
15 Chung, S., Gamcsik, M.P. and King, M.W., Biomed. Mater., 2011, 6(4): 045001
16 Zhao, Y. and Ding, J., Chinese. Sci. Bull., 2012, 57(2-3): 234
17 Flemming, R.G., Murphy, C.J., Abrams, G.A., Goodman, S.L. and Nealey, P.F., Biomaterials, 1999, 20(6): 573
18 Mata, A., Boehm, C., Fleischman, A.J., Muschler, G. and Roy, S., J. Biomed. Mater. Res., 2002, 62(4): 499
19 Berry, C.C., Campbell, G., Spadiccino, A., Robertson, M. and Curtis, A.S.G., Biomaterials, 2004, 25(26): 5781
20 Wan, Y.Q., Wang, Y., Liu, Z.M., Qu, X., Han, B.X., Bei, J.Z. and Wang, S.G., Biomaterials, 2005, 26(21): 4453
21 Khademhosseini, A., Langer, R., Borenstein, J. and Vacanti, J. P., Proc. Natl Acad. Sci. USA, 2006, 103(8): 2480
22 Charest, J.L., Eliason, M.T., Garcia, A.J. and King, W.P., Biomaterials, 2006, 27(11): 2487
23 Teixeira, A.I., McKie, G.A., Foley, J.D., Berticsc, P.J., Nealey, P.F. and Murphy, C.J., Biomaterials, 2006, 27(21): 3945
24 Sarkar, S., Lee, G. Y., Wong, J. Y. and Desai, T.A., Biomaterials, 2006, 27(27): 4775
25 Bettinger, C.J., Langer, R. and Borenstein, J.T., Angew. Chem. Int. Edit., 2009, 48(30): 5406
26 Mata, A., Kim, E.J., Boehm, C.A., Fleischman, A.J., Muschler, G.F. and Roy, S., Biomaterials, 2009, 30(27): 4610
27 Yao, L., Wang, S.G., Cui, W.J., Sherlock, R., O'Connell, C., Damodaran, G., Gorman, A., Windebank, A. and Pandit, A., Acta Biomater., 2009, 5(2): 580
28 Ghibaudo, M., Trichet, L., Le Digabel, J., Richert, A., Hersen, P. and Ladoux, B., Biophys. J., 2009, 97(1): 357
29 Zorlutuna, P., Elsheikh, A. and Hasirci, V., Biomacromolecules, 2009, 10(4): 814
30 Schulte, V.A., Diez, M., Moeller, M. and Lensen, M.C., Biomacromolecules, 2009, 10(10): 2795
31 Kantawong, F., Burgess, K.E.V., Jayawardena, K., Hart, A., Burchmore, R.J., Gadegaard, N., Oreffo, R.O.C. and Dalby, M.J., Biomaterials, 2009, 30(27): 4723
32 Kim, E.J., Boehm, C.A., Mata, A., Fleischman, A.J., Muschler, G.F. and Roy, S., Acta Biomater., 2010, 6(1): 160
33 Schulte, V.A., Diez, M., Hu, Y., Moeller, M. and Lensen, M.C., Biomacromolecules, 2010, 11(12): 3375
34 Tanaka, M., Biochim. Biophys. Acta, 2011, 1810: 251
35 Lopez-Alvarez, M., Pereiro, I., Serra, J., de Carlos, A. and Gonzalez, P., Biomed. Mater., 2011, 6(4): 045012

36 Pan, Z., Yan, C., Peng, R., Zhao, Y., He, Y. and Ding, J., Biomaterials, 2012, 33(6): 1730
37 Qu, Z. and Ding, J., Chinese. J. Chem., 2012, 30(10): 2257
38 Ishaug, S.L., Crane, G.M., Miller, M.J., Yasko, A.W., Yaszemski, M.J. and Mikos, A.G., J. Biomed. Mater. Res., 1997, 36(1): 17
39 Ma, P.X. and Choi, J.W., Tissue Eng., 2001, 7(1): 23
40 Wu, L.B. and Ding, J.D., Biomaterials, 2004, 25(27): 5821
41 Safinia, L., Wilson, K., Mantalaris, A. and Bismarck, A., Macromol. Biosci., 2007, 7(3): 315
42 Shen, H., Hu, X.X., Bei, J.Z. and Wang, S.G., Biomaterials, 2008, 29(15): 2388
43 Liu, Y.J., Jiang, H.L., Li, Y. and Zhu, K.J., Chinese. J. Polym. Sci., 2008, 26(1): 63
44 Pan, Z. and Ding, J., Interface Focus, 2012, 2(3): 366
45 Wu, L.B., Zhang, H., Zhang, J.C. and Ding, J.D., Tissue Eng., 2005, 11(7-8): 1105
46 Wu, L.B. and Ding, J.D., J. Biomed. Mater. Res. Part A, 2005, 75A(4): 767
47 Reignier, J. and Huneault, M.A., Polymer, 2006, 47(13): 4703
48 Odelius, K., Hoglund, A., Kumar, S., Hakkarainen, M., Ghosh, A.K., Bhatnagar, N. and Albertsson, A.C., Biomacromolecules, 2011, 12(4): 1250
49 Ma, Z.W., Gao, C.Y., Gong, Y.H. and Shen, J.C., J. Biomed. Mater. Res. Part B-Applied Biomat., 2003, 67B(1): 610
50 Zhang, J.C., Wu, L.B., Jing, D.Y. and Ding, J.D., Polymer, 2005, 46(13): 4979
51 Murphy, W.L., Dennis, R.G., Kileny, J.L. and Mooney, D.J., Tissue Eng., 2002, 8(1): 43
52 Shi, G.X., Wang, S.G. and Bei, J.Z., J. Funct. Polym., 2001, 14: 7
53 McBeath, R., Pirone, D.M., Nelson, C.M., Bhadriraju, K. and Chen, C.S., Dev. Cell, 2004, 6(4): 483
54 Peng, R., Yao, X., Cao, B., Tang, J. and Ding, J., Biomaterials, 2012, 33(26): 6008
55 Wang, Z., Zhang, Z., Zhang, J.C., She, Z.J. and Ding, J.D., Chinese Sci. Bull., 2009, 54(17): 2968
56 Goldstein, A.S., Juarez, T.M., Helmke, C.D., Gustin, M.C. and Mikos, A.G., Biomaterials, 2001, 22(11): 1279
57 Moroni, L. and Lee, L.P., J. Biomed. Mater. Res. Part A, 2009, 88A(3): 644
58 Hollister, S.J., Adv. Mater., 2009, 21(32-33): 3330